Supporting Information for"Coastal polynyas enable transitions between high and low West Antarctic ice shelf melt rates"

Ruth Moorman[1], Andrew F. Thompson[1], and Earle A. Wilson[2]

[1]Environmental Science and Engineering, California Institute of Technology, Pasadena, California, USA

[2]Department of Earth System Science, Stanford University, Stanford, California, USA

Contents of this file

1. Text S1 to S3

2. Figures S1 to S6

3. Table S1

Introduction The SI includes a summary of techniques used to analyze the historical observational data sets employed in this study (S1), the methods for deriving model parameters and forcing fields from the WAIS 1080 numerical output (S2, Figures S1-3), a brief summary of how the idealized model responds to parameter perturbations (S3, Figure S4), and two additional transiently forced simulations not included in the main text (Figures S5-6). We refer to Jupyter Notebooks, provided in linked GitHub repository (`https://github.com/ruth-moorman/Moorman-et-al-GRL-submission-2023`) accompanied by a binder environment so that readers can open, edit, and execute all code from a browser.

———

May 26, 2023, 10:48pm

Text S1.

Here we provide details of the γ and $\mathrm{AD_{mCDW}}$ metrics presented in Figure 1d.

Following Simpson, Allen, and Morris (1978) and Venables and Meredith (2014), we define the stratification metric γ as the potential energy of the water column relative to the potential energy of a mixed water column. This choice is made in lieu of buoyancy frequency metrics, which are found to be sensitive to an arbitrary choice of thermocline depth. The diagnosed potential energy is effectively the energy input required to homogenize the water column to a given depth. Functionally, this metric γ is defined as

$$\gamma = \int_{h_2}^{h_1} (\rho - \langle\rho\rangle)gz\,dz \quad \text{where} \quad \langle\rho\rangle = \frac{1}{h_2 - h_1}\int_{h_2}^{h_1} \rho\,dz. \tag{1}$$

We take h_1 to be a near surface depth (5 m) and h_2 to be a depth sufficiently deep to be typically located below the thermocline yet shallow enough so that the deepest measurement in at least half of the 49 profiles used in this study exceed h_2 (here 750 m). For a vertically mixed column, $\gamma = 0$ with γ growing increasingly positive for increasingly stable stratification. Only those profiles with a maximum depth exceeding h_2 are used in the calculation of γ, since the value of the integrated metric is artificially reduced by missing values. At least 2 profiles meet this criterion for each cruise year and the choice $h_2 = 750$ m. The temporal pattern is not sensitive to reasonable perturbations (up to and greater than 100 m) of h_1 and h_2. Interactive code used to compute this metric and test its sensitivity to h_1 and h_2 are available in the notebook "Figure1.ipynb" of the provider jupyter binder environment and GitHub repository.

Details of the metric used for the depth of the mCDW layer, $\mathrm{AD_{mCDW}}$, are provided in Kim et al. (2021) and the "Figure1.ipynb" notebook. The method simultaneously solves

for volume fractions of mCDW, WW, and glacial meltwater, comprising each point of a vertical profile of temperature, salinity, and dissolved oxygen given end member characteristics of the three water masses. Volume fractions are then vertically integrated and AD_{mCDW} is taken as the depth of the profile minus the integrated mCDW volume fraction. Thermocline depths calculated by this method are shallow biased relative to a visual identification of thermoclines identified from temperature profiles, as WW is modified by mCDW. However, the temporal pattern agrees with simpler methods based on isotherm depths. We choose to present AD_{mCDW} since isotherm based metrics were found to be sensitive to the choice of isotherm. All code and additional details (including methods of determining end member water mass characteristics) are available in "Figure1.ipynb" of the provided jupyter binder environment.

Text S2.

Here we describe how estimates of α, F_{surf}, and Ψ_{in} are diagnosed from WAIS 1080 output. Further details and interactive code generating these values and associated figures may be found in "Supplementary_2.ipynb".

Ice-shelf melt coefficient: α

In our idealized model, we parameterize the 2D transport of buoyancy (units $m^3 \ s^{-3}$) from the ice shelf cavity into the upper, thermocline box due to ice shelf melt as

$$h(vb)_{\text{in}} = \alpha \, h_{\text{mCDW}} \, \Delta b_{\text{melt}}. \qquad (2)$$

Using WAIS 1080 output, this 2D transport of buoyancy into the ocean thermocline box can be diagnosed as the total buoyancy transport to the ocean from basal ice shelf melt

$(\text{m}^4 \text{ s}^{-3})$ divided by the idealized model width (m),

$$h(vb)_{\text{in}} = \frac{1}{L_x} \int_A F_{\text{iceshelf}} \, dA. \tag{3}$$

Here L_x (m) is the model zonal extent, F_{iceshelf} ($\text{m}^2 \text{ s}^{-3}$) is the simulated buoyancy flux

from the ice shelf to the ocean within the ice shelf cavity at each horizontal grid point on

the ice shelf draft, and A is horizontal area of the ice shelf cavity (white box in Figure

S1). Combining Ficeshelf1 and Ficeshelf2, we estimate the value of the parameter α as,

$$\alpha = \frac{1}{L_x \, h_{\text{mCDW}} \, \Delta b_{\text{melt}}} \int_A F_{\text{iceshelf}} \, dA \tag{4}$$

where $L_x = 55$ km and $\Delta b_{\text{melt}} = 6.7 \times 10^{-3}$ m s^{-2} (as described in the main text), while

h_{mCDW} and the integrated buoyancy flux term are diagnosed from WAIS 1080.

The buoyancy flux F_{iceshelf} ($\text{m}^2 \text{ s}^{-3}$) is defined functionally as (positive values increase

the ocean buoyancy),

$$F_{\text{iceshelf}} = \frac{g\alpha_0}{\rho_{surf} c_p} Q_{H,\text{ice}} - g\beta_0 S_{surf} Q_{FW,\text{ice}} \tag{5}$$

where $g = 9.8$ m s^{-2} (gravity), $\alpha_0 = 4.8 \times 10^{-5}$ K^{-1} (thermal expansion coefficient),

$\beta_0 = 7.8 \times 10^{-4}$ (haline contraction coefficient), $c_p = 3992$ J kg^{-1} K^{-1} (specific heat

capacity of seawater), $\rho_{surf} = 1026$ kg m^{-3} (approximate surface cell density), $S_{surf} = 34$

(approximate surface cell salinity), $Q_{H,\text{ice}}$ = net heat flux from the ice (positive increases

θ) (WAIS 1080 output), and $Q_{FW,\text{ice}}$ = net freshwater flux from the ice (positive increases

S) (WAIS 1080 output). Figure S1 shows time mean WAIS 1080 F_{iceshelf} values for ice

shelves in the Amundsen Sea Embayment and delineates (white box) the Dotson Ice Shelf

horizontal region integrated over in alpha. Whilst the adjacent Dotson and Crosson ice

shelves are connected in WAIS 1080, there is negligible flow between them across the

eastern boundary of the delineated region. The mCDW layer thickness, h_{mCDW} (m), is approximated as the thickness below the 0°C thermocline, computed from temperature spatially averaged over the ice front region (red box in Figure S1). Figure S2 shows h_{mCDW} directly diagnosed from WAIS 1080 and approximated from the ice shelf buoyancy input via alpha with $\alpha = 0.0021$ (mean diagnosed value).

Polynya surface buoyancy flux: F_{surf}

The ocean surface buoyancy flux, F_{surf} (m^2 s^{-3}), is defined functionally as (positive values increase the buoyancy of the surface cell),

$$F_{surf} = \frac{g\alpha_0}{\rho_{surf}c_p}Q_{H,\mathrm{oce}} - g\beta_0 S_{surf}Q_{FW,\mathrm{oce}}, \tag{6}$$

where $Q_{H,\mathrm{oce}}$ = net surface heat flux (positive increases θ) (WAIS 1080 output), $Q_{FW,\mathrm{oce}}$ = net surface freshwater flux (positive reduces S) (WAIS 1080 output), and all other parameters are as in Ficeshelf. To generate monthly and climatological mean timeseries of F_{surf}, which provides forcing to the idealized model (Figure S3), F_{surf} is averaged over a 55 km × 50 km region at the ice front where negative F_{surf} values are concentrated. This region is delineated in Figure S2 (red box). Our results are not qualitatively sensitive to the exact size of this region, and these values are simply intended to guide the magnitude of forcing terms.

In the main text we refer to F_{surf} as the surface buoyancy flux associated with net sea-ice formation. As defined in Fsurf, F_{surf} is the total surface buoyancy flux, not purely the buoyancy flux associated with sea-ice formation and melt. However, F_{surf} is tightly anti-correlated ($R^2 = 0.96, p = 10^{-240}$, Figure S3) with monthly net sea-ice formation in WAIS 1080 and so, for clarity, we refer to F_{surf} as reflecting sea-ice formation.

:

Cross-shelf volume transport: Ψ_{in}

Ψ_{in} (units $\text{m}^2 \text{ s}^{-1}$) represents the net baroclinic shoreward transport of warm mCDW into the coastal region at the Dotson Ice Shelf front and the balanced offshore transport of cool thermocline waters. This term is estimated via a preliminary analysis of the Dotson Ice Front overturning circulation as simulated in WAIS 1080. We bin monthly mean volume transports across the edges of the ice front region (red box in Figure S1), and the corresponding monthly mean ocean temperature values, into surface referenced potential density (σ_0) bins using monthly mean σ_0 values. Density-binned volume transports into the ice front domain are then summed along the bounds of the box, whilst density-binned temperatures are averaged along the bounds of the box. When cumulatively integrated through σ_0 space, binned transports reveal a net shoreward flow of dense waters (interpreted as mCDW) and a net offshore flow of lighter waters (WW, glacial meltwater, and other surface waters), consistent with the assumptions of the model.

Text S2.

Analytical steady state solutions to the ice front overturning model

Analytical steady state solutions for the thickness of the thermocline layer and the thermocline stratification strengh in the ice front overturning model may be derived for known values of κ_{P},

$$h_{\text{steady}} = \left(\frac{H}{2} - \frac{\Psi_{\text{in}}}{2\alpha}\right) + \sqrt{\left(\frac{H}{2} - \frac{\Psi_{\text{in}}}{2\alpha}\right)^2 + \frac{\kappa_{\text{P}} L}{\alpha}} \tag{7}$$

$$\Delta b_{\text{steady}} = \frac{\left(h_{\text{steady}} - \frac{\Psi_{\text{in}}}{\alpha}\right)\left(\frac{F_{\text{surf}} L}{2\Psi_{\text{in}}} + \Delta b_{\text{melt}}\right)}{\frac{\kappa_{\text{P}} L}{2\Psi_{\text{in}}} + \frac{H}{2} - \frac{\Psi_{\text{in}}}{\alpha}} - \Delta b_{\text{melt}}. \tag{8}$$

Interpretation of these solutions is complicated by the Δb dependence of κ_{P} (see equation (10) of the main text). To understand (7) and (8) in light of this dependence, consider the extreme case of taking $\phi \to \infty$ in equation (10) of the main text , which reverts κ_{P} to a step function transitioning from κ_{diff} to κ_{conv} when Δb drops below Δb_{crit}. In this case, (7) and (8) suggest two steady states for a given system $(H, L, \alpha, \Delta b_{\mathrm{melt}})$ and forcing $(\Psi_{\mathrm{in}}, F_{\mathrm{surf}})$; a diffusive steady state with $\kappa_{\mathrm{P}} = \kappa_{\mathrm{diff}}$ and a convective steady states with $\kappa_{\mathrm{P}} = \kappa_{\mathrm{conv}}$. In some regions of the forcing space, one of these κ_{P} values present a contradiction. Either setting $\kappa_{\mathrm{P}} = \kappa_{\mathrm{diff}}$ will result in $\Delta b_{\mathrm{steady}} < \Delta b_{\mathrm{crit}}$ (indicating the diffusive solution is not sustained, white regions in Figure 3b,c of the main text) or setting $\kappa_{\mathrm{P}} = \kappa_{\mathrm{conv}}$ results in $\Delta b_{\mathrm{steady}} > \Delta b_{\mathrm{crit}}$ (indicating the convective solution is not sustained, white regions in Figure 3d,e of the main text). Where neither κ_{P} value returns a contradiction, bistability is possible (region bound by yellow contour in Figure 3b-e of the main text). Smoothing the transition between κ_{diff} and κ_{conv}, by decreasing the value of ϕ, primarily acts to constrict the region over which bistability is possible. Numerical solutions presented in Figure 3 of the main text agree with analytical solutions (central panels of Figure S4), though they differ in that the numerical bistable region is contracted relative to the analytical bistable region, as anticipated for nonzero values of ϕ.

Summary of parameter sensitivity

These analytical solutions provide a fast and convenient means of exploring the sensitivity of model output to parameter choices. "Supplementary_3.ipynb" in the provided jupyter binder environment generates analytical versions of Figure 3 (main text) for the full suite of possible cases wherein each model parameter is both positively and negatively perturbed. Figure S4 illustrates the model steady state sensitivity to changes in α as an

example; all other cases are available in the provided notebook. Table S1 summarizes the effects of varying each parameter, both on the analytical steady state solutions (explored in the jupyter notebok) and on transiently forced simulations (not shown). The positive feedbacks and related bistablity underpinning our main results depend on their being a nonlinearity to the dependence of vertical mixing on stratification strength. Within the confines of our choice to represent vertical mixing as a smoothed step function of stratification strength, we find that parameter perturbations can change the absolute magnitude of the thermocline depths associated with diffusive and convective conditions, can alter the length of the simulated lag between thermocline depth and stratification strength changes during regime transitions, and can change the strength of forcing perturbation required to trigger a regime transition. Small perturbations to the parameter values used in this study do not alter our key results, however, removing the jump in vertical mixing strength at the onset of convection does remove the described behavior.

References

Kim, T.-W., Yang, H. W., Dutrieux, P., Wåhlin, A. K., Jenkins, A., Kim, Y. G., ... Cho, Y.-K. (2021). Interannual Variation of Modified Circumpolar Deep Water in the Dotson-Getz Trough, West Antarctica. *Journal of Geophysical Research: Oceans*, *126*(12), e2021JC017491.

Simpson, J., Allen, C., & Morris, N. (1978). Fronts on the continental shelf. *Journal of Geophysical Research: Oceans*, *83*(C9), 4607–4614.

Venables, H. J., & Meredith, M. P. (2014). Feedbacks between ice cover, ocean stratification, and heat content in ryder bay, western antarctic peninsula. *Journal of Geophysical Research: Oceans*, *119*(8), 5323–5336.
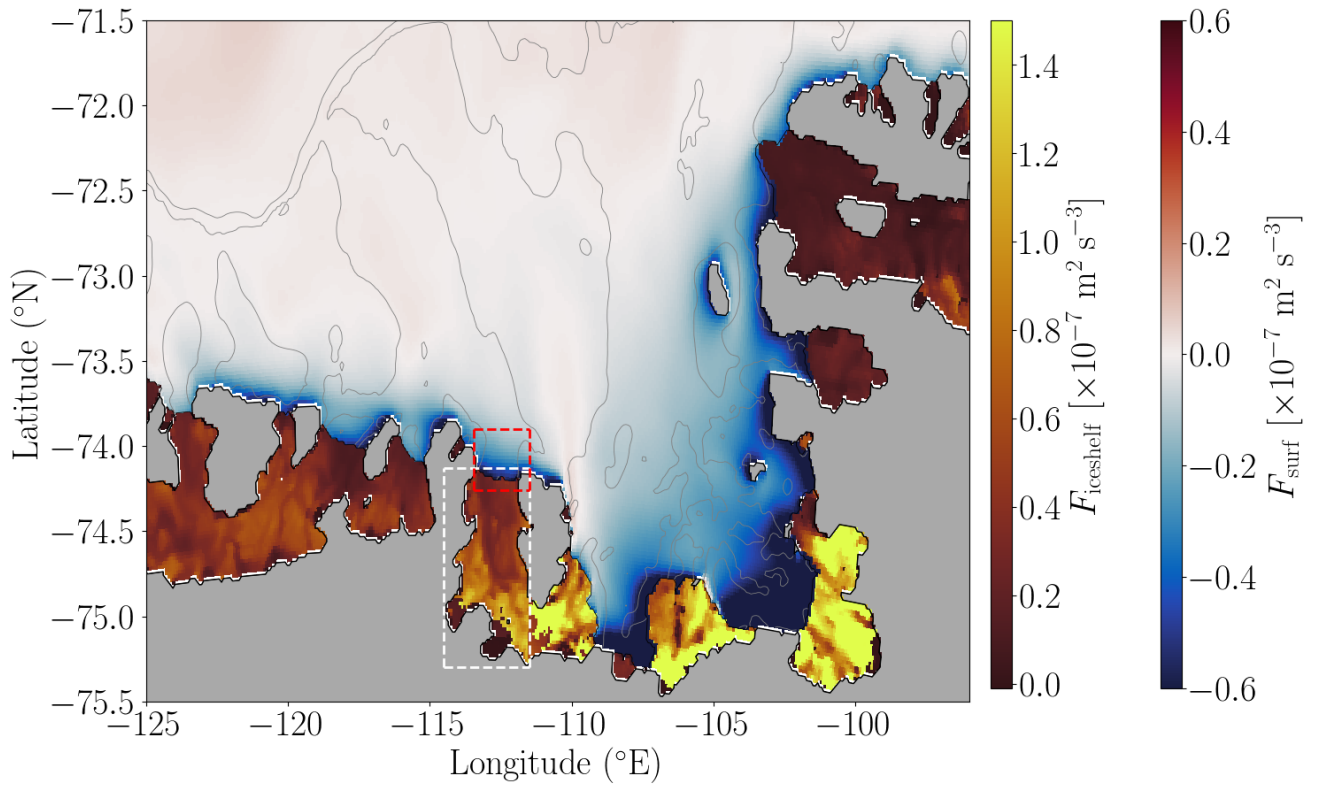
Figure S1. Time mean $F_{iceshelf}$ and F_{surf} values from WAIS 1080 diagnosed according to equations Ficeshelf and Fsurf. $F_{iceshelf}$ is defined for regions with positive ice shelf draft and F_{surf} is defined for regions of open ocean (zero ice shelf draft). The grounded ice zone is delineated with grey shading. Grey contours in the open ocean indicate bathymetry (500 m, 1000 m, 4000 m). The white dashed box indicates the region over which $F_{iceshelf}$ is computed (the Dotson Ice Shelf) and the red dashed box indicates the region over which F_{surf}, Ψ_{in}, and h_{mCDW} are computed (the Dotson Ice Front).

May 26, 2023, 10:48pm

:
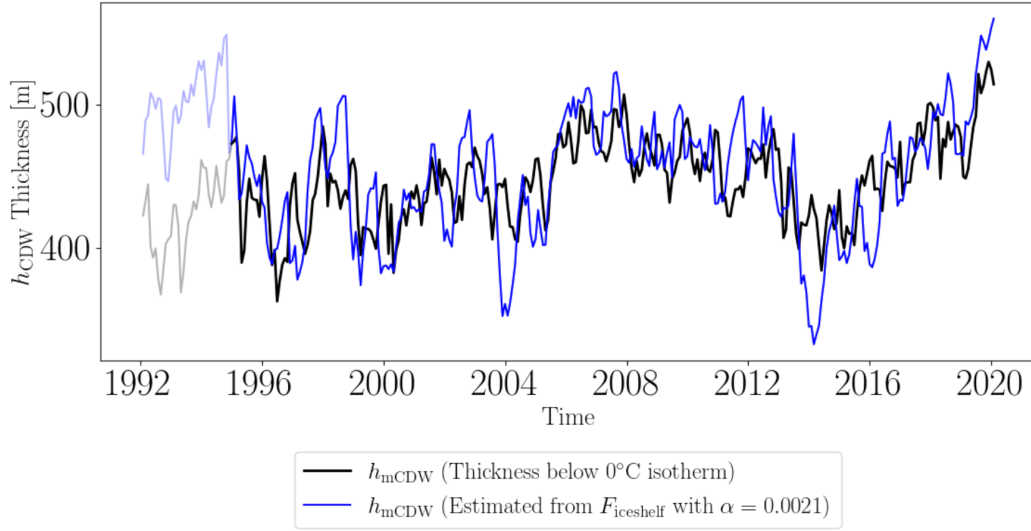
Figure S2. Timeseries of h_{mCDW} defined as either the thickness below the 0°C isotherm determined from monthly WAIS 1080 temperature output spatially averaged over the ice front region (black), or a linear function of spatially integrated Dotson Ice Shelf buoyancy fluxes (see equation Ficeshelf) with α set to 0.0021 (blue). The first three years (translucent lines) show worse agreement between the direct and parameterized h_{mCDW} values, possibly a result of model spinup.
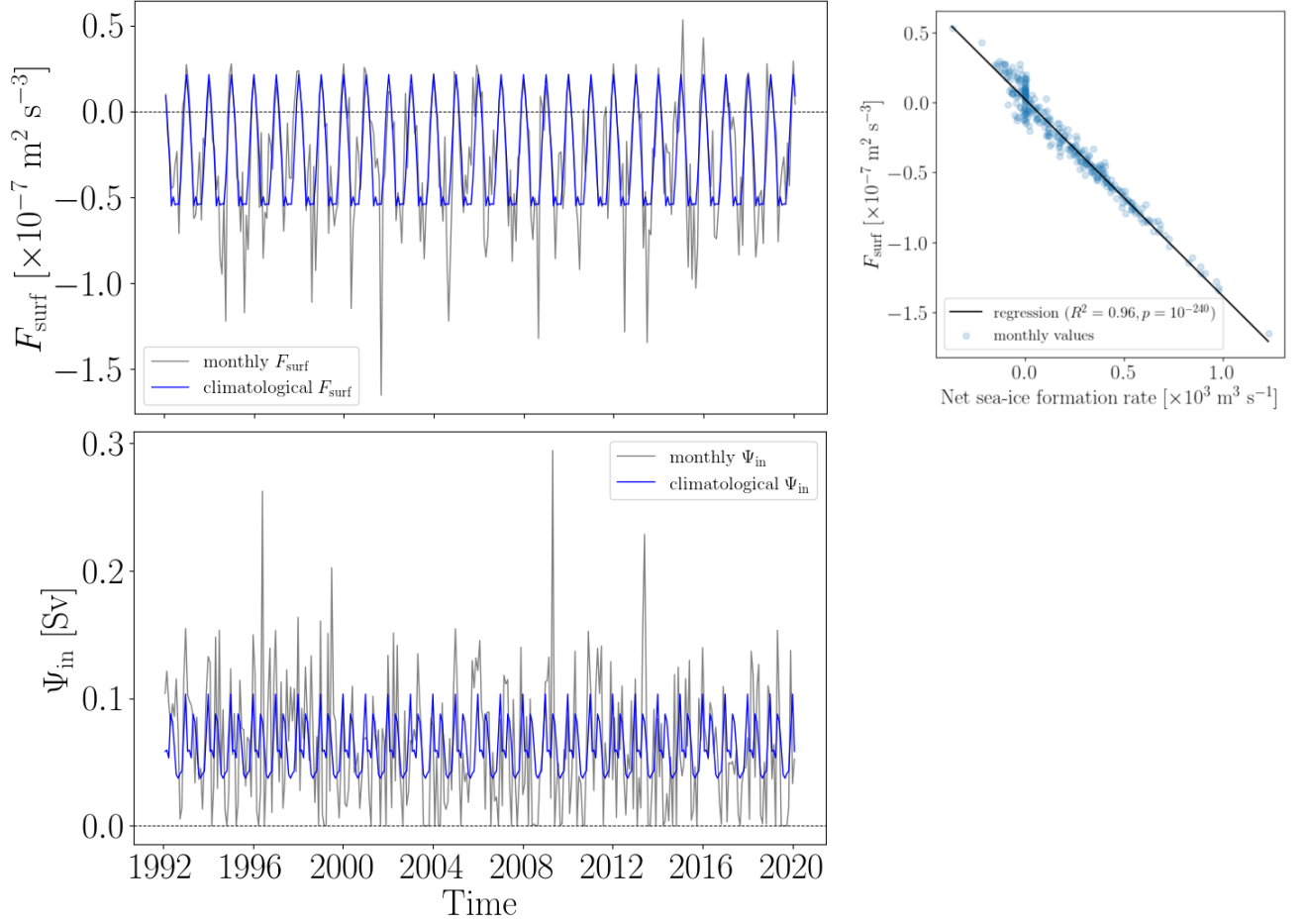
Figure S3. Monthly mean values (grey) and climatological mean monthly values (blue) of F_{surf} (upper) and Ψ_{in} (lower) as diagnosed from WAIS 1080. (right) Correlation between F_{surf} and monthly net sea-ice formation rates in the Dotson ice front region.
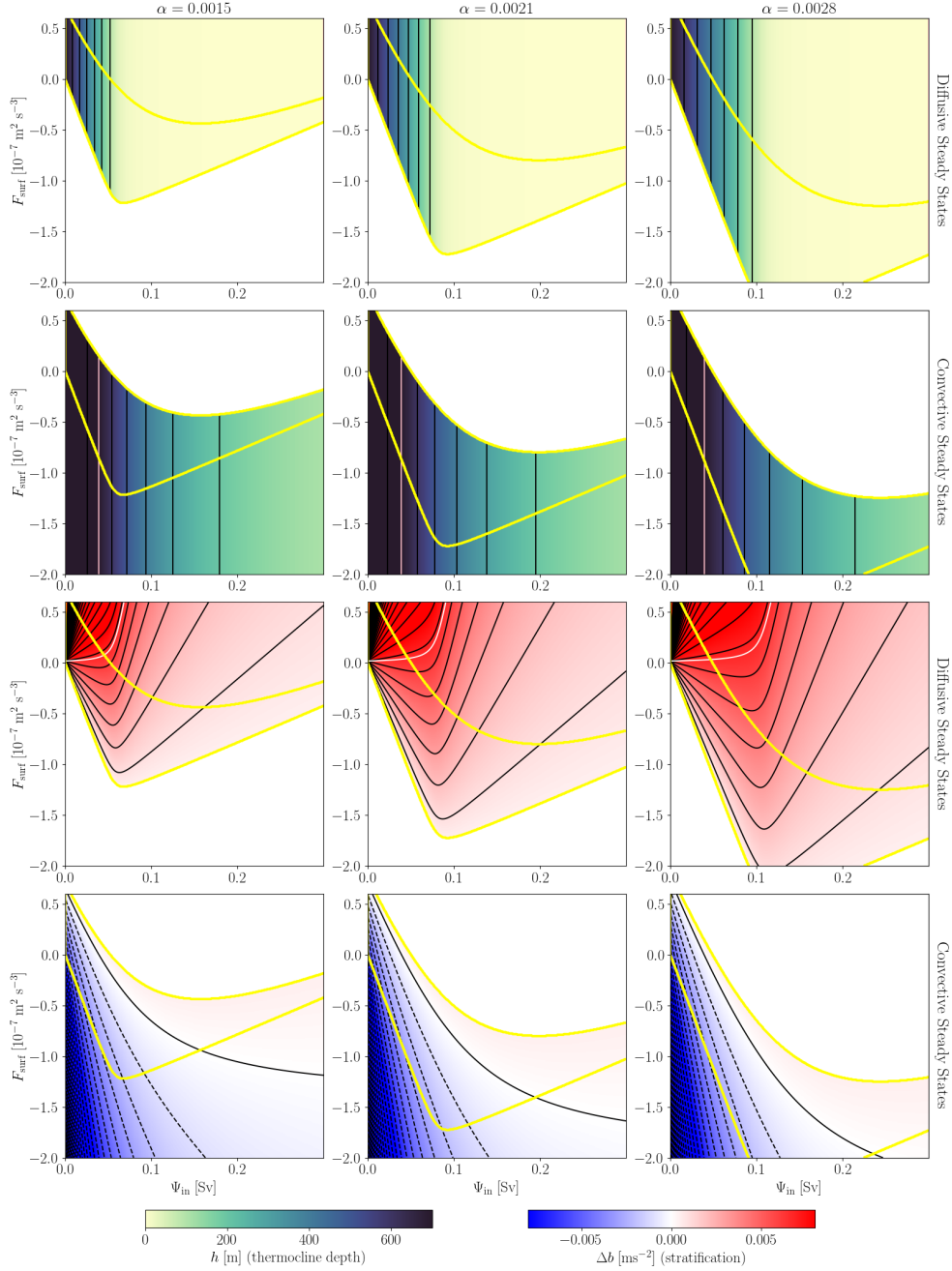
Figure S4. Illustration of the sensitivity of analytical steady-state solutions to perturbations of the parameter α. Each column contains panels equivalent to Figure 3b-e of the main text, except analytical solutions rather than numerically equilibrated solutions are shown. The central column shows analytical steady-state solutions to our model when the default (main text) parameter values are used (these panels may be directly compared to Figure 3b-e). Columns to the left and right show analytical steady-state solutions when α is reduced and increased, respectively.
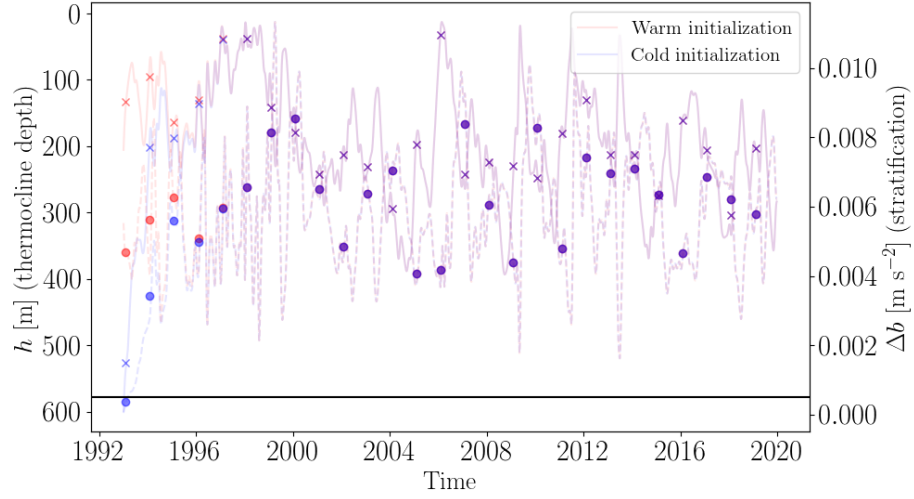
Figure S5. Thermocline depth changes and stratification strength changes simulated in response to monthly (as opposed to climatological) WAIS 1080 forcing. The same forcing is applied to the model initialized in warm conditions (red) and cold conditions (blue). Crosses, circles, solid lines, and dashed lines are as in Figure S6. Black horizontal line is Δb_{crit}, stratification strength does not drop below this value following initialization.

May 26, 2023, 10:48pm
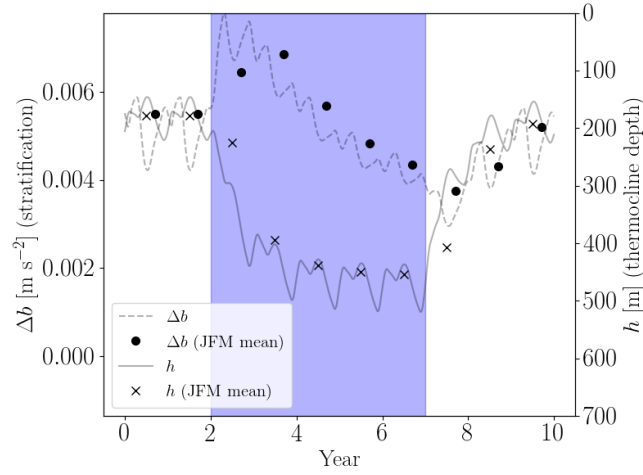
Figure S6. Similar to Figure 4d for the main text. In Figure 4d, winter (May-September) Ψ_{in} values are shifted downwards for two consecutive years. Here the full annual pattern of Ψ_{in} is downshifted (by the same amount as in Figure 4d, the maximum offset that ensures $\Psi_{\mathrm{in}} > 0$) for 5 consecutive years. Whilst this forcing pattern generates large decadal scale fluctuations in the thermocline depth, it does not trigger regime change as the accompanying stratification changes do not promote the onset of convection.

Table S1. Dominant effects of increasing the magnitude of a parameter on the analytical steady state solutions to the ice front overturning model and the implied effect on transiently forced solutions. Effects of decreasing parameter magnitudes are the converse in all cases.

Parameter	Effect (analytical steady state)	Implied Effect (transient)
α	α dictates the sensitivity of meltwater generation to the thickness of the ice front mCDW layer. Increasing α acts to: - strengthen the ice front stratification associated with a given thermocline depth - deepen the steady state thermocline associated with a given mCDW inflow - shift the bistable region towards negative F_{surf} values (see Figure S3.1)	Stronger perturbations are needed to force diffusive to convective transitions and weaker perturbations are sufficient to force convective to diffusive transitions. Both convective and diffusive solutions are associated with deeper thermoclines.
Δb_{melt}	Δb_{melt} similarly dictates the sensitivity of ice front stratification strength to basal ice melt. It has a similar effect to α except it only influences steady state stratification strengths, not steady state thermocline depths.	Same as α, except does not effect end member thermocline depths.
κ_{diff}	κ_{diff} only effects diffusive end member solutions and increasing it acts to: - deepen the steady state thermocline associated with diffusive end members - contract the bistable region from below such that diffusive solutions are not supported for a wider range of negative F_{surf} values (when $\kappa_{\mathrm{diff}} = \kappa_{\mathrm{conv}}$ bistability disappears altogether as the end member solutions converge)	Diffusive solutions are associated with deeper thermoclines generally and transitions to convective solutions are possible with weaker perturbations.
κ_{conv}	κ_{conv} only effects convective end member solutions and increasing it acts to: - deepen the steady state thermocline associated with convective end members - expand the bistable region from above such that convective solutions are supported for a wider range of positive F_{surf} values (when κ_{diff} and κ_{conv} become more similar bistability contracts, when κ_{diff} and κ_{conv} become more different bistability expands)	Convective solutions are associated with deeper thermoclines generally and transitions to diffusive solutions require stronger perturbations.
Δb_{crit}	Simply changes the stratification strength at which convection onsets. Increasing Δb_{crit} will shift the bistable region towards positive F_{surf} values.	Stronger perturbations are needed to force convective to diffusive transitions and weaker perturbations are sufficient to force diffusive to convective transitions.
ϕ^{a}	Increasing ϕ makes κ_{P} more step-like, therefore bringing the numerical model behavior closer to the analytical solution. Decreasing ϕ, by contrast, smooths out κ_{P}. This renders more solutions with steady state stratification strength close to the critical buoyancy unstable, and thus contracts the bistable region.	Transitions will require greater perturbations when ϕ is larger.

[a] analytical solutions are independent of ϕ, its effect has been assessed using numerical solutions